

Construction of two-dimensional hydrogen clusters on Au(111) directed by phthalocyanine molecules

Kai Yang, Wende Xiao, Liwei Liu, Xiangmin Fei, Hui Chen, Shixuan Du, and Hong-Jun Gao (✉)

Institute of Physics, Chinese Academy of Sciences, Beijing 100190, China

Received: 26 August 2013
Revised: 19 September 2013
Accepted: 21 September 2013

© Tsinghua University Press
and Springer-Verlag Berlin
Heidelberg 2013

KEYWORDS

hydrogen,
manganese phthalocyanine,
Au(111),
interfacial phase,
scanning tunneling
microscopy

ABSTRACT

Low-dimensional H₂ aggregates have been successfully fabricated on Au(111) surfaces and investigated by means of low temperature scanning tunneling microscopy. We use manganese phthalocyanine (MnPc) molecules anchored on the Au(111) surface to efficiently collect and pin hydrogen molecules. A two-dimensional (2D) molecular hydrogen cluster is formed around the MnPc. The hydrogen cluster exhibits bias-dependent topography and spatial-dependent conductance spectra, which are rationalized by the exponentially decreasing threshold energy with distance from the central MnPc to activate the motion of the H₂ molecules. This exponential drop reveals an interfacial phase behavior in the 2D cluster.

1 Introduction

Molecular hydrogen is widely used today in many of the largest-volume chemical reactions, all involving H₂ catalytic activation [1]. Hydrogen is a diatomic molecular solid at low pressures and temperatures, with strong covalent molecular bonds and weak intermolecular interactions [2]. Solid hydrogen is also an archetypal quantum solid, characterized by free rotational states, strong quantum behavior of its nuclei and large intermolecular anharmonicity [2]. Hydrogen in reduced dimensions may behave quite differently

from the bulk because intermolecular attractions can be weakened [3–5]. Low-dimensional H₂ aggregates may reveal rich quantum phenomena and are optimal for practical reasons as different materials interact via their surface/boundary, particularly in heterocatalysis. However, due to its low melting temperature and high molecular diffusivity, it is difficult to fabricate low-dimensional H₂ aggregates. This difficulty has hindered the investigation of their structural and electronic properties, the results of which may shed new insight on the understanding of the surface structure as well as the quantum properties of solid hydrogen.

Address correspondence to hjgao@iphy.ac.cn

Solid surfaces provide a unique platform for fabrication of novel low-dimensional structures, enabling direct access of scanning tunneling microscopy (STM) in real space for exploration of structural and electronic properties [6, 7]. Previous STM studies have revealed that H₂ molecules form a close-packed monolayer with a hexagonal lattice after intensive dosage of H₂ gas on Cu(111) at low temperature (5 K) [8, 9]. However, to the best of our knowledge, no low-dimensional nanostructure of H₂ on a solid surface has been prepared and imaged in real space, due to the high mobility of H₂ molecules.

In this work, we have successfully prepared two-dimensional (2D) hydrogen clusters on Au(111) surfaces and investigated their structural and electronic properties by means of low-temperature scanning tunneling microscopy (LT-STM). First, we deposited manganese phthalocyanine (MnPc) molecules on Au(111) to act as nucleation centers. When subsequently dosed onto the surface, hydrogen molecules self-assemble into 2D clusters around the MnPc molecules. The 2D clusters exhibit topographic evolution with bias voltages, in line with their spatial-dependent conductance spectra. This novel behavior is rationalized by the spatial-dependent energy barriers required to change the adsorption conformations of the hydrogen molecules, revealing an interfacial phase behavior. Our work demonstrates that foreign organic molecules can be introduced to efficiently pin and collect hydrogen molecules on a surface, which facilitates the fabrication of low-dimensional H₂ aggregates and exploration of their novel physical properties and possible applications.

2 Experimental

Experiments were carried out in an ultrahigh vacuum (base pressure of 1×10^{-10} mbar) LT-STM system (Unisoku), equipped with standard surface processing facilities. An atomically flat Au(111) surface was prepared by repeated cycles of Ar⁺ sputtering and annealing. Commercial MnPc molecules (Sigma-Aldrich, 97% purity) were sublimated from a Knudsen-type evaporator after thermal purification, while the Au(111) substrate was held at room temperature. The sample was then transferred *in situ* into the LT-STM

head held at 4.2 K. Hydrogen molecules (99.999% purity) were then admitted to the sample surface by flooding the chamber where the LT-STM head was located to a pressure of 5×10^{-7} mbar for 100 min. We expect that the hydrogen molecules were cold prior to the adsorption on the gold surface, since direct line of sight from the ultrahigh vacuum chamber to the sample surface is long (about 1.2 m) and blocked by a shutter held at 4.2 K. STM images were acquired in the constant-current mode, and all given voltages refer to the sample. Differential conductance (dI/dV) spectra were collected by using a lock-in technique with a 5 mV_{rms} sinusoidal modulation at a frequency of 973 Hz. All measurements were performed at 4.2 K with electrochemically etched tungsten tips, which were calibrated against the surface state of the Au(111) surface before spectroscopic measurements.

3 Results and discussion

The fabrication of 2D hydrogen clusters using MnPc anchored on Au(111) is schematically shown in Fig. 1(a). The MnPc molecule consists of a central Mn²⁺ ion and a macrocycle of alternating carbon and nitrogen atoms, exhibiting four-fold symmetry [10–12]. At low coverage, MnPc molecules are predominantly adsorbed at the elbow sites of the $22 \times \sqrt{3}$ reconstruction of Au(111) surfaces [13–15]. Prior to hydrogen dosage, each MnPc molecule exhibits a cross-like structure (Fig. 1(b)). The protrusion at the center of the MnPc molecule originates from the d_{z^2} orbitals of the central Mn²⁺ ion, while the lobes are assigned to the four benzene rings (Fig. 1(b)) [10, 16]. Interestingly, we observe a depressed periphery of each MnPc molecule after exposure to H₂ at a sample temperature of 4.2 K (Fig. 1(c)). The boundary of the dark area is a four-fold symmetric trench around the MnPc molecule (Fig. 1(c)), reflecting the symmetry of the MnPc molecule.

To clarify the detailed structure of the depressed peripheries of the MnPc molecules, we collect STM images of the periphery of a single MnPc with a series of bias voltages. As shown in Fig. 2, the width of the trench becomes narrower and nearly undistinguishable at a bias voltage of -40 mV (Fig. 2(g)). Meanwhile, with decreasing bias voltages a halo develops and extends from the central MnPc. Round protrusions

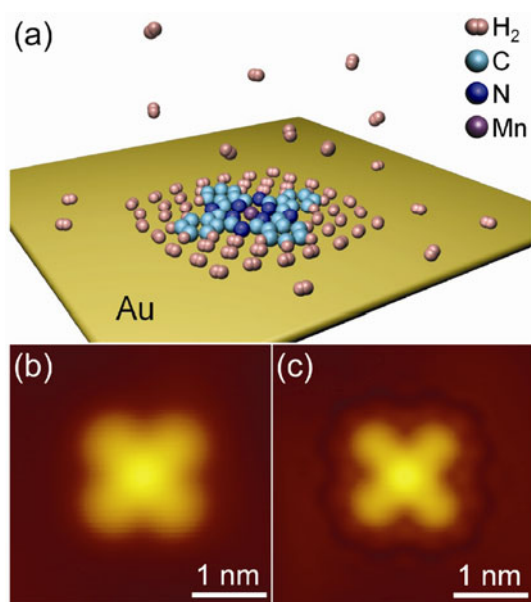


Figure 1 Construction of 2D hydrogen cluster on Au(111). (a) Schematic of the fabrication of 2D hydrogen cluster using an MnPc molecule on Au(111). MnPc anchored on Au(111) surface serves as nucleation center to efficiently collect and pin hydrogen molecules. (b) STM image of single MnPc molecule prior to hydrogen dosage. (c) STM image of single MnPc molecule after hydrogen dosage at a sample temperature of 4.2 K. The dark trench around the MnPc molecule indicates the condensates of hydrogen molecules. Scanning parameters: (b) sample bias $U = -200$ mV, tunneling current $I = 10$ pA; (c) $U = -200$ mV, $I = 200$ pA.

can be identified in the halos. We attribute the round protrusions to hydrogen molecules, as the temperature for hydrogen molecules to decompose on Au films is ~ 80 K [11, 17], much higher than the sample temperature in our experiments. The condensed hydrogen molecules tend to form a 2D hexagonal lattice (Figs. 2(g)–2(i)) and the average separation between the hydrogen molecules around the central MnPc is ~ 3.8 Å, akin to that of bulk solid hydrogen [2, 8]. The MnPc molecules thus act as nucleation centers to collect and pin the hydrogen molecules (Fig. 1(a)). The apparent heights of hydrogen molecules decrease with increasing distance from the central MnPc, as revealed by the line profile analysis (Fig. 3(b)). In addition, the hydrogen molecules far from the central MnPc are arranged loosely compared to those close to MnPc (Fig. 3(a)). For instance, the separation between the hydrogen molecules labeled as 1 and 2 in Fig. 3(a) is ~ 3.5 Å, while the distance increases to ~ 4.3 Å for the ones labeled as 2 and 3 (Fig. 3(b)).

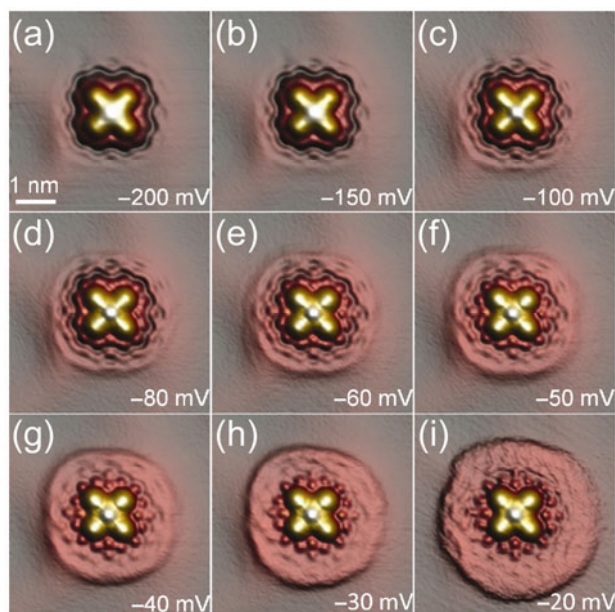


Figure 2 Topographic evolution of the 2D hydrogen cluster with sample bias. (a)–(i) STM images of the 2D hydrogen cluster around the central MnPc with varying sample bias. The width of the trench becomes smaller with decreasing bias voltage and nearly disappears in (g). A halo develops and becomes larger in radius. The hydrogen molecules are clearly identified as round protrusions inside the halo in (d)–(i). Scanning parameters: sample bias is indicated in the figure, $I = 200$ pA, 5.5 nm \times 5.5 nm.

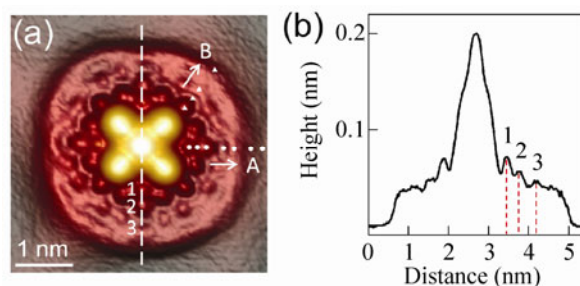


Figure 3 Arrangement and height of hydrogen molecules in the cluster. (a) High resolution STM image (scanning parameters: $U = -40$ mV, $I = 200$ pA, 4.5 nm \times 4.5 nm) showing a 2D hydrogen cluster around the central MnPc molecule. White dots and triangles represent the positions where dI/dV spectra were collected. (b) Line profile along the dashed line in (a).

Figures 4(a) and 4(b) show the differential conductance (dI/dV) spectra collected along two directions (A and B shown in Fig. 3(a)) of the 2D H₂ cluster. Two symmetric dips located at about ± 55 meV (indicated by black arrows) and a small dip at zero bias (zero bias anomaly) are displayed in the uppermost (purple) curve in Fig. 4(a). Similar features can be identified in other dI/dV spectra shown in Figs. 4(a) and 4(b).

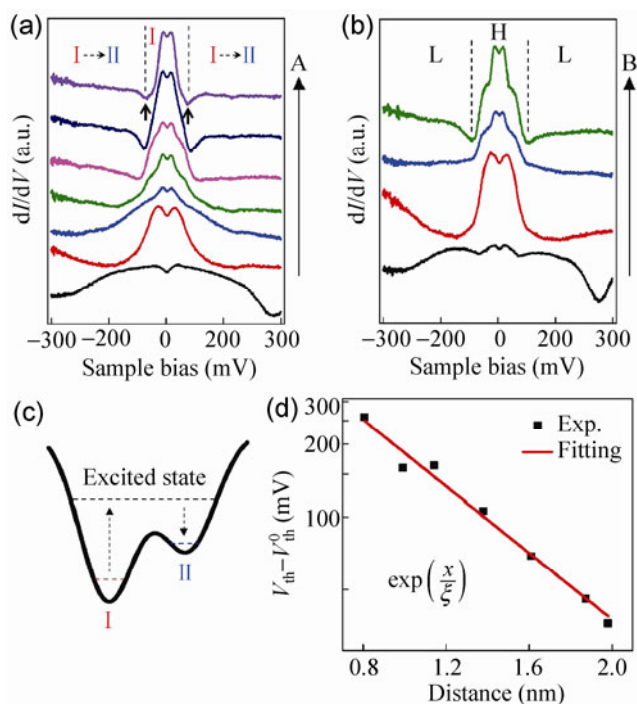


Figure 4 Spatial-dependent dI/dV spectra taken on the 2D hydrogen cluster. (a) dI/dV spectra (setpoint: $I = 200$ pA, $U = -200$ mV) taken along the A (dots) direction in Fig. 3(a). The spectra from bottom to top are measured from the center towards the edge, and are vertically displaced for clarity. Black arrows pointing at the symmetric dips indicate the threshold voltage for transition between different conductance states. (b) dI/dV spectra (setpoint: $I = 200$ pA, $U = -200$ mV) taken along the B (triangles) direction in Fig. 3(a). The system can lie in a high (H) or low (L) conductance state separated by V_{th} . (c) Two-level-system model for hydrogen molecule in the STM junction. Above the threshold voltage, the hydrogen molecule can be vibrationally excited from the ground state (state I) and relax into the other energy minimum (state II), resulting in conduction dips in dI/dV spectra (see for example, the dips indicated by the black arrows in the uppermost (purple) curve in (a)). (d) Dependence of V_{th} on distance (x) from the central Mn^{2+} ion along the A direction in Fig. 3(a) (logarithmic plot), demonstrating an exponential decay (error bars vary from 0.18 to 0.98, which are too small to be displayed). The red line shows the exponential fit. V_{th}^0 is a fitting constant with dimensions of voltage. The inverse of ξ (0.63 nm \pm 0.2 nm) represents the decay rate of V_{th} with distance.

The dips and zero bias anomaly in the dI/dV spectra suggest that the system possesses complex dynamics at certain biases. Similar dynamic behavior has been described by the two-level-system (TLS) model [8, 18–21]. A TLS has two nearly degenerate states, separated by a large potential barrier (shown schematically in Fig. 4(c)). The inelastically scattered tunneling electrons can inject energy into the system,

switching the internal degree of freedom of the system between the two states with low and high conductance. The hydrogen molecules in the STM junction can lie in two adsorption states with different conductances, which can be treated as a TLS. Tunneling electrons can excite the hydrogen molecules at the threshold voltages (V_{th}), giving rise to an abrupt change in fractional occupations of the high and low conductance states, which results in the conductance dips in dI/dV spectra in Figs. 4(a) and 4(b) [8, 21, 22]. The nearly symmetric alignment of V_{th} with respect to zero bias indicates that the excitation is a vibrational process [23, 24]. Normally, the conductance dips will exhibit a negative value [8, 18, 22], which is not the case in our data. One possible reason is that the sweep rate of the voltage when taking dI/dV spectra is not quick enough to follow the abrupt change in the fractional occupation of the two states, so that the discontinuity of the conductance change is smoothed by taking time average.

The zero bias anomaly can be attributed to a voltage induced non-equilibrium occupation of the two nearly degenerate states of the TLS [25, 26]. Alternatively, it has been proposed that the fast TLS (here “fast” means that quantum tunneling rate of the system between the two states is in the range of 1 mK to 10 K determined by the uncertainty principle) may show a Kondo anomaly [27]. Here the spin-flip process of the normal magnetic Kondo problem is replaced by an electron-assisted transition between the two states of the TLS [20, 26]. However, the exact origin of the zero bias anomaly remains controversial [18, 26].

The bias-dependent topography of the 2D H_2 cluster is directly related to its spatial-dependent electronic structures. As seen in Figs. 4(a) and 4(b), a hydrogen molecule can stay in different conductance states depending on the bias voltages. For instance, the uppermost (green) curve in Fig. 4(b) shows two different conductance states. The hydrogen molecule will stay in the high conductance state (indicated by “H”) when the bias voltage is lower than the V_{th} \sim 70 mV. Once the applied bias voltage exceeds this critical value, the molecule will be excited to the low conductance state with a high probability (indicated by “L”). The critical value of V_{th} decreases with increasing separation from the central MnPc (Figs. 4(a)

and 4(b)). Thus, the hydrogen molecules far from the central MnPc can only be resolved when the bias voltage is low enough during STM image acquisition. The lower the applied bias voltage, the more hydrogen molecules can be clearly resolved. The increasing activation bias to the high conductance state from the inside to the outside of the halo underlies the bias-dependent topography of the 2D H₂ cluster around the MnPc molecule as shown in Fig. 2.

We have already shown that the hydrogen molecules far from the central MnPc molecule are arranged loosely compared to those close to the MnPc molecule (Fig. 3). As the molecular packing of hydrogen is mainly driven by van der Waals interactions, the larger intermolecular separation suggests a weaker interaction between hydrogen molecules. Thus, the energy barriers to be overcome in order to change the adsorption conformations of hydrogen molecules in the 2D clusters decrease from the center to the boundary of the 2D clusters, which rationalizes the spatial-dependent evolution of the dI/dV spectra shown in Figs. 4(a) and 4(b).

The hydrogen molecular clusters around the MnPc molecules from the inside to the outside of the halo may be viewed as an interfacial phase between 2D solid and 2D fluid. The tightly packed hydrogen molecules close to the central MnPc correspond to the solid phase. Away from the center, the spatial ordering of H₂ molecules becomes weaker and these H₂ molecules are not so well distinguished from each other, leading to blurred protrusions in the STM images (Fig. 2). The nearly uncorrelated H₂ molecules at the edge of, and outside, the halo represent the fluid phase.

Statistically, the transition from one phase to another occurs at a surface only one or two molecules thick [28]. Molecules at the interface are bounded on two sides by entirely different environments and the intermolecular forces tend to pull them toward a bulk phase. A typical example is a droplet of water, which tends to assume a spherical shape to minimize the surface area. In the 2D H₂ cluster, the value of V_{th} reflects the strength of the intermolecular forces and the correlations of the H₂ molecules with others at a certain location. As shown in Fig. 4(d), the measured V_{th} has an exponential dependence on the distance from

the central MnPc molecule. This exponential decay reflects the quasi-long-range order in the 2D H₂ cluster, i.e., the nearby correlations between H₂ molecules decay rapidly at large distances.

4 Conclusions

We have demonstrated that 2D H₂ clusters, formed around MnPc molecules anchored on Au(111), exhibit bias-dependent topography and spatial-dependent conductance spectra. The 2D H₂ clusters can be viewed as an interfacial phase between 2D solid and 2D fluid. The threshold voltage to activate the motion of the H₂ molecules decreases exponentially with distance from the central MnPc, reflecting the quasi-long-range order in the 2D H₂ clusters. Our results demonstrate that foreign organic molecules can efficiently collect and pin H₂ molecules on a surface. The resulting 2D hydrogen clusters provide platforms to investigate their novel properties and the chemical reactions of hydrogen on solid surfaces.

Acknowledgements

This work was financially supported by the National Natural Science Foundation of China (Nos. 51210003 and 11290165), National Basic Research Program of China (No. 2009CB929103), TRR61 and Chinese Academy of Sciences.

References

- [1] Chopra, I. S.; Chaudhuri, S.; Veyan, J. F.; Chabal, Y. J. Turning aluminium into a noble-metal-like catalyst for low-temperature activation of molecular hydrogen. *Nat. Mater.* **2011**, *10*, 884–889.
- [2] Mao, H.-K.; Hemley, R. J. Ultrahigh-pressure transitions in solid hydrogen. *Rev. Mod. Phys.* **1994**, *66*, 671–692.
- [3] Halperin, W. P. Quantum size effects in metal particles. *Rev. Mod. Phys.* **1986**, *58*, 533–606.
- [4] Qin, S. Y.; Kim, J.; Niu, Q.; Shih, C.-K. Superconductivity at the two-dimensional limit. *Science* **2009**, *324*, 1314–1317.
- [5] Brun, C.; Hong, I. P.; Patthey, F.; Sklyadneva, I. Y.; Heid, R.; Echenique, P. M.; Bohnen, K. P.; Chulkov, E. V.; Schneider, W.-D. Reduction of the superconducting gap of ultrathin Pb islands grown on Si(111). *Phys. Rev. Lett.* **2009**,

- 102, 207002.
- [6] Crommie, M. F.; Lutz, C. P.; Eigler, D. M. Confinement of electrons to quantum corrals on a metal surface. *Science* **1993**, *262*, 218–220.
- [7] Loth, S.; Baumann, S.; Lutz, C. P.; Eigler, D. M.; Heinrich, A. J. Bistability in atomic-scale antiferromagnets. *Science* **2012**, *335*, 196–199.
- [8] Gupta, J. A.; Lutz, C. P.; Heinrich, A. J.; Eigler, D. M. Strongly coverage-dependent excitations of adsorbed molecular hydrogen. *Phys. Rev. B* **2005**, *71*, 115416.
- [9] Lotze, C.; Corso, M.; Franke, K. J.; von Oppen, F.; Pascual, J. I. Driving a macroscopic oscillator with the stochastic motion of a hydrogen molecule. *Science* **2012**, *338*, 779–782.
- [10] Lu, X.; Hipps, K. W. Scanning tunneling microscopy of metal phthalocyanines: d^6 and d^8 cases. *J. Phys. Chem. B* **1997**, *101*, 5391–5396.
- [11] Liu, L. W.; Yang, K.; Jiang, Y. H.; Song, B. Q.; Xiao, W. D.; Li, L. F.; Zhou, H. T.; Wang, Y. L.; Du, S. X.; Ouyang, M.; et al. Reversible single spin control of individual magnetic molecule by hydrogen atom adsorption. *Sci. Rep.* **2013**, *3*, 1210.
- [12] Liu, L. W.; Yang, K.; Xiao, W. D.; Jiang, Y. H.; Song, B. Q.; Du, S. X.; Gao, H. J. Selective adsorption of metal-phthalocyanine on Au(111) surface with hydrogen atoms. *Appl. Phys. Lett.* **2013**, *103*, 023110-5.
- [13] Barth, J. V.; Brune, H.; Ertl, G.; Behm, R. J. Scanning tunneling microscopy observations on the reconstructed Au(111) surface: Atomic structure, long-range superstructure, rotational domains, and surface defects. *Phys. Rev. B* **1990**, *42*, 9307–9318.
- [14] Yokoyama, T.; Yokoyama, S.; Kamikado, T.; Okuno, Y.; Mashiko, S. Selective assembly on a surface of supramolecular aggregates with controlled size and shape. *Nature* **2001**, *413*, 619–621.
- [15] Xiao, W.; Ruffieux, P.; Ait-Mansour, K.; Gröning, O.; Palotas, K.; Hofer, W. A.; Gröning, P.; Fasel, R. Formation of a regular fullerene nanochain lattice. *J. Phys. Chem. B* **2006**, *110*, 21394–21398.
- [16] Jiang, Y. H.; Xiao, W. D.; Liu, L. W.; Zhang, L. Z.; Lian, J. C.; Yang, K.; Du, S. X.; Gao, H.-J. Self-assembly of metal phthalocyanines on Pb(111) and Au(111) surfaces at submonolayer coverage. *J. Phys. Chem. C* **2011**, *115*, 21750–21754.
- [17] Stobiński, L.; Duś, R. Molecular hydrogen chemisorption on thin unsintered gold films deposited at low temperature. *Surf. Sci.* **1993**, *298*, 101–106.
- [18] Temirov, R.; Soubatch, S.; Neucheva, O.; Lassise, A. C.; Tautz, F. S. A novel method achieving ultra-high geometrical resolution in scanning tunnelling microscopy. *New J. Phys.* **2008**, *10*, 053012.
- [19] Ralph, D. C.; Buhrman, R. A. Observations of Kondo scattering without magnetic impurities: A point contact study of two-level tunneling systems in metals. *Phys. Rev. Lett.* **1992**, *69*, 2118–2121.
- [20] Halbritter, A.; Borda, L.; Zawadowski, A. Slow two-level systems in point contacts. *Adv. Phys.* **2004**, *53*, 939–1010.
- [21] Thijssen, W. H. A.; Djukic, D.; Otte, A. F.; Bremmer, R. H.; van Ruitenbeek, J. M. Vibrationally induced two-level systems in single-molecule junctions. *Phys. Rev. Lett.* **2006**, *97*, 226806.
- [22] Gaudioso, J.; Lauhon, L. J.; Ho, W. Vibrationally mediated negative differential resistance in a single molecule. *Phys. Rev. Lett.* **2000**, *85*, 1918–1921.
- [23] Stipe, B. C.; Rezaei, M. A.; Ho, W. Single-molecule vibrational spectroscopy and microscopy. *Science* **1998**, *280*, 1732–1735.
- [24] Smit, R. H. M.; Noat, Y.; Untiedt, C.; Lang, N. D.; van Hemert, M. C.; van Ruitenbeek, J. M. Measurement of the conductance of a hydrogen molecule. *Nature* **2002**, *419*, 906–909.
- [25] Kozub, V. I.; Rudin, A. M.; Schober, H. R. Adiabatic electron renormalization of dynamical defects and point contact resistance anomalies. *Solid State Commun.* **1995**, *95*, 415–419.
- [26] von Delft, J.; Ralph, D. C.; Buhrman, R. A.; Upadhyay, S. K.; Louie, R. N.; Ludwig, A. W. W.; Ambegaokar, V. The 2-channel Kondo model: I. Review of experimental evidence for its realization in metal nanoconstrictions. *Ann. Phys.–New York* **1998**, *263*, 1–55.
- [27] Cox, D. L.; Zawadowski, A. Exotic Kondo effects in metals: Magnetic ions in a crystalline electric field and tunnelling centres. *Adv. Phys.* **1998**, *47*, 599–942.
- [28] Luo, J.; Cheng, H.; Asl, K. M.; Kiely, C. J.; Harmer, M. P. The role of a bilayer interfacial phase on liquid metal embrittlement. *Science* **2011**, *333*, 1730–1733.